World Journal of Engineering and Technology, 2022, 10, 230-240
https://www.scirp.org/journal/wjet
ISSN Online: 2331-4249
ISSN Print: 2331-4222

Analysis of Factors Affecting Sealing Performance of Subsea Wellhead Connector

Liangliang Ding, Miao Xian

School of Mechanical and Electrical Engineering, Southwest Petroleum University, Chengdu, China
Email: lld1210@qq.com

How to cite this paper: Ding, L.L. and Xian, M. (2022) Analysis of Factors Affecting Sealing Performance of Subsea Wellhead Connector. *World Journal of Engineering and Technology*, **10**, 230-240.
https://doi.org/10.4236/wjet.2022.102014

Received: February 28, 2022
Accepted: May 7, 2022
Published: May 10, 2022

Abstract

Subsea wellhead connector is the key equipment for offshore oil and gas production. The working water depth is generally more than 500 m, so it has higher requirements for its sealing performance. In this paper, the VX gasket matched with H-4 subsea wellhead connector is taken as the research object, and the mechanical analysis under preload and production conditions is carried out. The finite element model of subsea wellhead connector is established by ABAQUS software, and the influence of axial preload, production pressure and material properties on the sealing performance of VX gasket is studied. The results show that the greater the axial preload, the greater the contact stress on the gasket surface; the contact stress decreases first and then increases linearly with the increase of production pressure; the material properties of the gasket are also an important factor affecting its sealing performance, 316L stainless steel is more suitable for gasket material than 304 stainless steel and Inconel625.

Keywords

Subsea Connector, Sealing Performance, VX Gasket, Contact Stress, Finite Element Analysis

1. Introduction

Subsea wellhead connector is usually installed between the Christmas tree and the subsea high-pressure wellhead to prevent the leakage of high temperature and high-pressure fluid in the well and the infiltration of seawater in the oil and gas production process [1] [2]. Once it leaks, it can cause accidents such as blowout [3]. Therefore, studying the connection strength and sealing performance of subsea wellhead connector under various working conditions can avoid catastrophic accidents caused by sealing failure and improve the efficiency and safety of offshore oil and gas production [4].

At present, the research on the sealing performance of subsea wellhead connector has been reported, but there are shortcomings. Rao [5] carried out tracking experiment and improvement on VX gasket, and explored its sealing principle. Li *et al.* [6] proposed a new type of metal seal structure by optimizing the sealing surface angle, which effectively reduced the installation preload force, and verified the superiority of the structure by prototype experiments. Wang and Zhu [7] studied the relationship between components and parameters through the established three-dimensional finite element model, and explored the structural performance and sealing performance of subsea wellhead connectors under different working modes. Tang *et al.* [8] analyzed the sealing performance of subsea wellhead connector under preload, production and different bending moment conditions by establishing two-dimensional axisymmetric model. Zeng *et al.* [9] proposed that the sealing contact strength as the evaluation index of sealing performance of VX gasket is more accurate than the contact stress.

The above research provides some supporting evidence for the design and application of subsea wellhead connector, but the influence of gasket material properties on the sealing performance of VX gasket is not considered. Therefore, ABAQUS software is used to analyze the sealing performance of subsea wellhead connector under preload and production conditions, and the influence of axial preload, production pressure and gasket material properties on its contact stress is explored, in order to provide basis for the sealing structure design of other types of subsea wellhead connector.

2. Connector Structure and Working Principle

Subsea wellhead connector is the key equipment to connect the subsea high pressure wellhead with the subsea Christmas tree and prevent the leakage of high temperature and high-pressure fluid in the well. It is faced with extremely bad load, so it has higher requirements for its sealing performance. As shown in **Figure 1**, the subsea wellhead connector is mainly composed of VX gasket, locking block, driving ring, and subsea high-pressure wellhead [10].

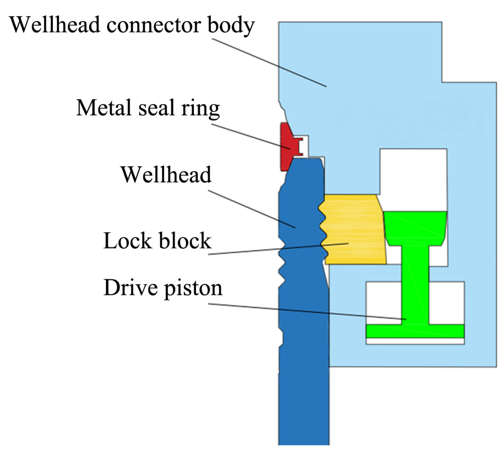

Figure 1. Structural diagram of wellhead connector.

When preloaded, the driving ring squeezes the lock block downward under the action of locking hydraulic pressure, making it mesh with the subsea wellhead to achieve locking. When unlocking, the driving ring is driven upward under the action of hydraulic pressure, and the lock block is released. The spring between the lock blocks separates the lock block from the meshing surface of the subsea wellhead.

3. Establishment of Mathematical Model of Connector

3.1. Structure and Mechanical Analysis of VX Gasket

The target wellhead is the H-4 standard subsea wellhead with the inner diameter of 476.25 mm ($18\frac{3}{4}$ in) and the outer diameter of 685.8 mm (27 in). Under the production conditions, the internal pressure needs to be about 103 MPa. The structure of the supporting VX gasket is shown in Figure 2. The corresponding structural parameters are shown in Table 1.

3.2. Seal Determination Basis

When preloaded, gasket sealing surface contact stress should be greater than the sealing pressure (y = 179.3 MPa); under production conditions, the contact stress of gasket sealing surface is three times greater than the internal pressure p [11].

3.3. Mechanical Analysis of Preloaded Condition

When preloaded, the force diagram of VX gasket is shown in Figure 3. Because its structure and force are symmetrical, only the upper surface is taken for analysis.

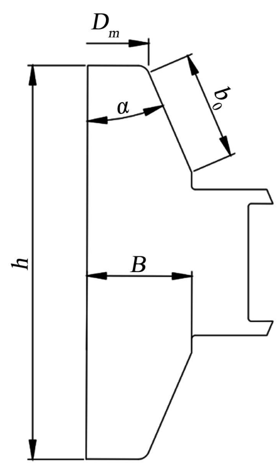

Figure 2. Structure size of VX gasket.

Table 1. Structural parameters of VX gasket.

D_m/mm	h/mm	B/mm	b_0/mm	α/(°)
510	102	26.2	30	23

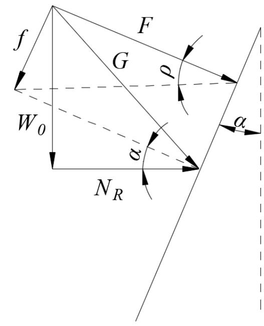

Figure 3. Force diagram of gasket under preload.

Under the preloaded condition, the lock block moves downward to drive the tree, and then preloaded the VX gasket. The normal pressure on the sealing surface is:

$$F = \pi D_m b q_0 \quad (1)$$

where, D_m is the diameter of the gasket, mm; b is average width of contact surface, mm; q_0 is the contact surface pressure under preload, MPa, and q_0 is at least the sealing specific pressure.

The gasket has upward movement trend relative to the sealing groove, so the friction f on the sealing surface is downward, and the resultant force G with the compression force F is:

$$G = \frac{\pi D_m b q_0}{\cos \rho} \quad (2)$$

where, ρ is the friction angle between the gasket and the sealing groove, and $\rho = 8.5^\circ$ when steel contacts with steel.

G can be decomposed into axial preloaded force W_0 and rebound force N_R generated by compression of the gasket. The force on a single-sealing surface is $N_R/2$:

$$W = \frac{\pi D_m b q_0}{\cos \rho} \sin(\alpha + \rho) \quad (3)$$

$$\frac{N_R}{2} = \frac{\pi D_m b q_0}{\cos \rho} \cos(\alpha + \rho) \quad (4)$$

where, α is gasket taper.

When the preloaded is completed, the is compressed to the maximum. When the radial compression is 2Δ, the circumferential strain ε_θ and circumferential stress σ_θ of the gasket are:

$$\varepsilon_\theta = \frac{\pi(D_m - 2\Delta) - \pi D_m}{\pi D_m} = -\frac{2\Delta}{D_m} \quad (5)$$

$$\sigma_\theta = E_R \varepsilon_\theta = -E_R \frac{2\Delta}{D_m} \quad (6)$$

where, E_R is the elastic modulus of the gasket material, MPa. The circumferential static equilibrium force diagram of the gasket is shown in **Figure 4**, and the static equilibrium can be obtained as follows:

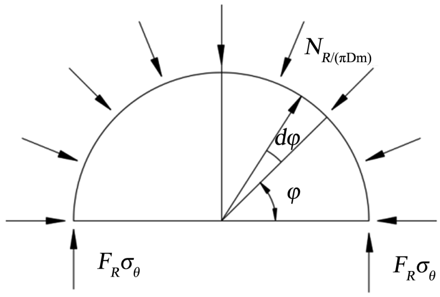

Figure 4. The circumferential static equilibrium of gasket.

$$\int_0^{\pi} \frac{N_R}{\pi D_m} R_m \sin\varphi \mathrm{d}\varphi = -2F_R\sigma_\theta = 2F_R E_R \frac{2\Delta}{D_m} \tag{7}$$

where: F_R is the cross-sectional area of the gasket, mm^2; R_m is the middle diameter of 1/2, mm; φ is the angle between the resilience per unit circumferential length and the gasket section.

The relationship between N_R and σ_θ:

$$N_R = \frac{4\pi E_R F_R \Delta}{D_m} \tag{8}$$

The above formula represents the rebound force caused by the radial deformation of 2Δ of the gasket, and the relationship between the contact surface pressure and the radial deformation is obtained [12]:

$$q_0 = \frac{2E_R F_R \Delta}{D_m^2 b} \frac{\cos\rho}{\cos(\alpha+\rho)} = \frac{W_0}{\pi D_m b} \frac{\cos\rho}{\sin(\alpha+\rho)} \tag{9}$$

Therefore, under the preloaded condition, the axial preloaded force W_0 or the radial compression Δ plays a decisive role in the contact stress of the sealing surface, and the contact stress is proportional to both.

3.4. Mechanical Analysis of Production Conditions

Under the production condition, due to the pressure of the internal channel of the connector, the connector has an upward trend. At this time, the axial force of the connector can be divided into four parts: the axial preloaded force W_0 under the preloaded condition, the axial load W_1 caused by the internal pressure on the connector and the axial load W_2 caused by the internal pressure on the inner diameter of the gasket, and the axial load W_3 caused by the radial compression of the gasket after rebound. This paper only gives a brief derivation process, please refer to reference [13] for the specific derivation process.

1) The axial load W_1 caused by internal pressure on the connector is:

$$W_1 = pS_p \tag{10}$$

where, p is the internal pressure, MPa; S_p is the area of connector under internal pressure, mm^2.

2) The axial load W_2 generated by the internal pressure acting on the inner diameter of the gasket is:

$$W_2 = \frac{1}{2}\pi D_m hp\tan(\alpha-\rho) \tag{11}$$

3) The force analysis is the same as that of preloaded. Assuming that the radial compression of the gasket under internal pressure is Δ_1, the axial load W_3 generated by the radial compression of the gasket after rebound is:

$$W_3 = \frac{2\pi F_R E_R \Delta_1}{D_m}\tan(\alpha-\rho) \tag{12}$$

Therefore, the reverse resultant force of the axial preload on the connector under production conditions is:

$$\begin{aligned} W_\Sigma &= W_1 + W_2 + W_3 \\ &= pS_p + \frac{1}{2}\pi D_m hp\tan(\alpha-\rho) + \frac{2\pi F_R E_R \Delta_1}{D_m}\tan(\alpha-\rho) \end{aligned} \tag{13}$$

With the gradual increase of internal pressure, the effect of axial force generated by internal pressure offsets part of the axial preload first, and the pressure value is:

$$p_{\min} = \frac{W_0}{\frac{1}{2}\pi D_m h\tan(\alpha-\rho) + s_p} \tag{14}$$

After reaching the minimum value, with the increase of internal pressure, the connector has an upward movement trend. After the internal pressure is applied, the radial deformation of the gasket changes from Δ at pretightening to Δ_1, and the deformation δ is:

$$\delta = \Delta - \Delta_1 \tag{15}$$

The deformation ΔL of the connector due to the axial action of the internal pressure is, and can be obtained from the relationship between ΔL and δ:

$$\Delta_1 = \Delta - \Delta L\tan\alpha = \Delta - \left(pS_p + W'' - W_0\right)\frac{L_1}{E_1 f_1}\tan\alpha \tag{16}$$

Therefore, the contact pressure q of the contact surface of the gasket under the production condition is:

$$\begin{aligned} q = {} & \frac{\left[\frac{1}{2}\pi D_m h - \frac{2\pi F_R E_R L_1 S_p}{D_m E_1 f_1}\tan\alpha\right]p + \frac{2\pi F_R E_R}{D_m}\left(\Delta + \frac{W_0 L_1}{E_1 f_1}\tan\alpha\right)}{1 + \frac{2\pi F_R E_R L_1}{D_m E_1 f_1}\tan(\alpha-\rho)\tan\alpha} \\ & \times \frac{\cos\rho}{\pi D_m b\cos(\alpha-\rho)} \end{aligned} \tag{17}$$

where, E_1 is the elastic modulus of connector material, MPa; L_1 is the length of the elongation part of the connector, mm; f_1 is the cross-sectional area of the connector elongation component, mm^2.

4. Finite Element Analysis

4.1. Finite Element Mesh Model

Because the structure and force of VX gasket are axisymmetric, a two-dimensional axisymmetric model of connector-wellhead system is established to simplify the calculation. All the components adopt CAX4R grid element type [14]. When meshing, the gasket cone surface and the sealing groove contact surface are meshed to ensure the accuracy of finite element analysis. The simplified finite element model and the mesh model are shown in Figure 5.

4.2. Material Properties

The Christmas tree, connector and wellhead are made of 8630 alloy steel, and VX gasket is made of Inconel 625 alloy steel. The materials and properties of the connector components are shown in Table 2.

4.3. Analysis Steps and Loading Boundary Conditions

According to the actual situation, this paper sets two analysis steps: preloaded condition and internal pressure condition. The first analysis step simulates the preloaded compression without medium pressure, and the preloaded force of the connector is applied to the tree. The second analysis step applied the medium pressure inside the connector (the pressure was 1.5 times of the rated pressure, p = 155 MPa);

Two contact pairs are set on the friction surface of the metal gasket and the seal groove, and the tangential behavior is defined by the penalty function. The friction coefficient is 0.15.

In order to limit the overall large displacement of the model, the fixed constraints in x and y directions are applied to the lower surface of the subsea wellhead. The tree body is set to binding constraints with wellhead and connector.

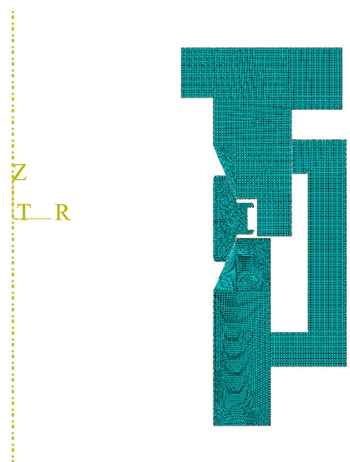

Figure 5. Finite element model of wellhead connector.

Table 2. Physical properties of materials.

Material	Yield strength (MPa)	Elastic modulus (GPa)	Poisson's ratio
8630	758	210	0.3
625	400	205	0.3

4.4. Analysis of Finite Element Results

4.4.1. Effect of Preload on Sealing Performance

The relationship between preloaded force and contact stress of contact surface under preloaded condition is analyzed by ABAQUS software, and compared with the theoretical value, as shown in Figure 6. The figure shows that when the preload is less than 1000 KN, the theoretical value is close to the analytical value, and the error is small. With the increase of preload, the contact stress increases slowly and less than the theoretical value. The reason is that in theoretical calculation, elastic analysis is adopted, assuming that the sealing ring is rigid body without deformation, while in finite element analysis, with the increase of preload, the contact area increases, leading to a decrease in contact stress.

4.4.2. Effect of Internal Pressure on Sealing Performance

Figure 7 shows the change curve of contact stress with the increase of internal pressure when the axial preload is 1853 KN.

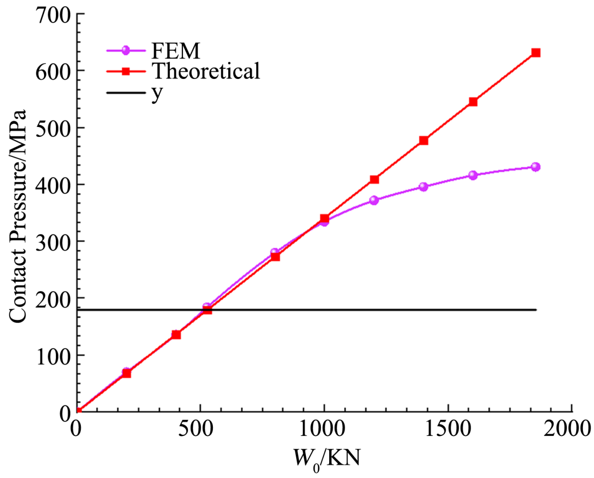

Figure 6. Relationship between axial preload and contact stress.

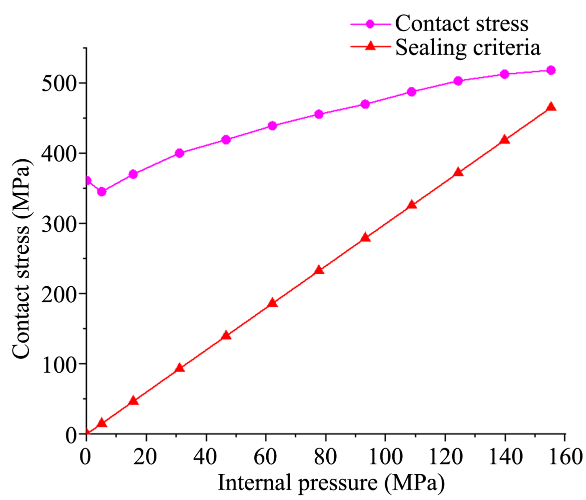

Figure 7. The relationship between internal pressure and contact stress under preload at 1853 KN.

As shown in Figure 7, with the increase of internal pressure, the contact stress first decreases and then increases. This is because the internal fluid pressure acting on the inner diameter channel of the connector will produce an upward axial load, which offsets part of the previous axial preload. At this time, the contact stress reaches the minimum. Then, with the continuous increase of internal pressure, the gasket is squeezed on the contact surface of the sealing groove to form a self-tightening seal, and the contact stress increases linearly.

Compared with the sealing criteria three times the sealing pressure value, the contact stress is greater than the judgment standard value, and the connector sealing performance is good, but eventually with the internal pressure continues to increase, the judgment standard line will intersect with the contact stress curve, at this time the seal will fail.

4.4.3. Effect of Material Properties on Sealing Performance

The material performance of VX gasket is also a factor affecting its sealing performance. By adding real stress-strain data, the distribution law of contact stress of 304 stainless steel, 316L stainless steel and Inconel625 alloy steel under internal pressure is analyzed, and the cloud chart of contact stress analysis is shown in Figure 8.

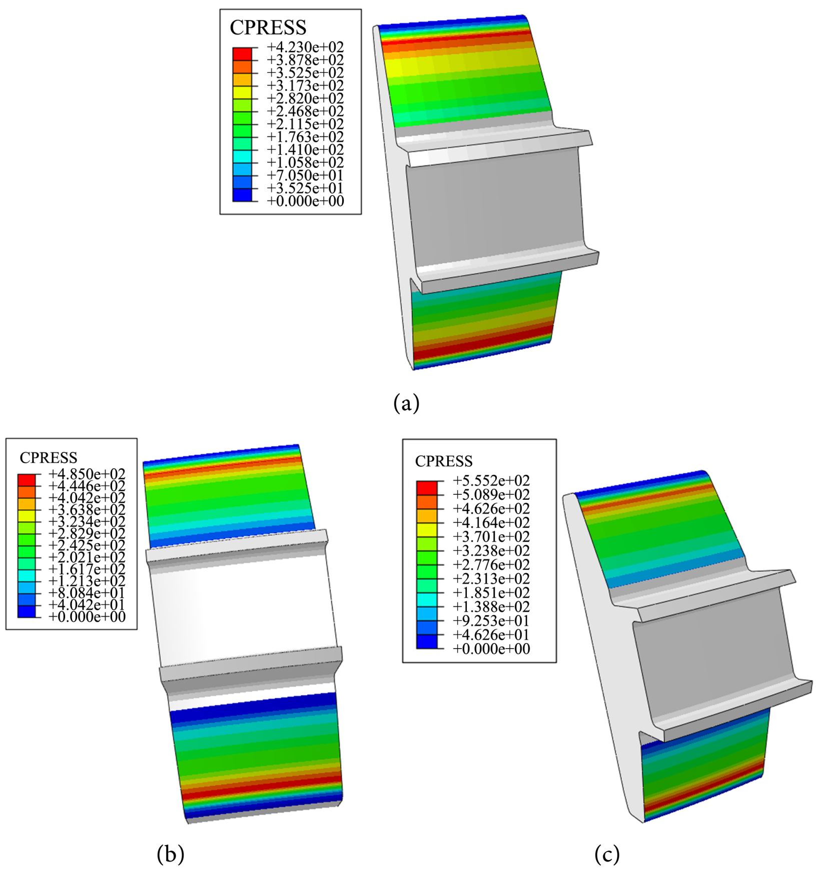

Figure 8. Contact stress contour of gasket with different materials. (a) Contact stress of 304 stainless steel material; (b) Contact stress of 316L stainless steel material; (c) Contact stress of Inconel625 alloy steel material.

Figure 8 shows the contact stress nephogram of different materials when the axial preload is 1853 KN and the internal pressure is 155 MPa. It can be seen from the figure that as the yield strength of the material increases, the effective contact width of the gasket decreases, and the maximum contact stress increases. The maximum contact stress of 304 stainless steel is 423 MPa, less than 465.0 MPa, so leakage may occur. The maximum contact stress of 316L stainless steel is less than that of Inconel625 alloy steel, but it has met the sealing criterion. Plastic deformation has occurred in the gasket under internal pressure conditions, and plastic deformation can better play its sealing role. Gasket is one-time vulnerable part, multiple-use will reduce its sealing performance, and Inconel625 alloy steel price is more expensive. Considering the above factors, it is more economical to use 316L stainless steel as the material of VX metal gasket under the requirements of sealing criteria.

5. Conclusions

1) An axisymmetric finite element model of H-4 connector was established to analyze its sealing performance under preload and internal pressure conditions.

2) On the premise of ensuring the structural strength of the connector, the preload force should be increased as far as possible. With the increase of internal pressure, the contact stress decreases first and then increases linearly.

3) 316L stainless steel is more suitable than 304 stainless steel and Inconel625 as gasket material.

Conflicts of Interest

The authors declare no conflicts of interest regarding the publication of this paper.

References

[1] Larson, E.D. and Keosoff, K.G. (2004) Marginal Subsea Development with Existing Subsea Trees. *Paper Presented at the Offshore Technology Conference*, Houston, Texas, May 2004, Paper Number: OTC 16533. https://doi.org/10.4043/16533-MS

[2] Qin, R., Gu, Y.H., Luo, X.L., *et al.* (2012) Parametric Analysis for the Design of Subsea Christmas Tree. *The Ocean Engineering*, **30**, 116-122.

[3] Chen, X.F., Zhao, H.L., Luo, X.L., *et al.* (2014) Study on Mechanical Properties of the VX Gasket of Subsea Horizontal Christmas Tree Wellhead Connector. *China Petroleum Machinery*, **42**, 62-67.

[4] Wang, J., Luo, X.L., Duan, M.L., *et al.* (2013) Research of Subsea X-Tree Wellhead Connector's Locking Mechanism. *Oil Field Equipment*, **42**, 16-21.

[5] Rao, S.H. (1998) A Study on the Sealing Principle of VX steel Ring. *China Offshore Platform*, No. 4, 30-33.

[6] Li, Z.G., Yun, F.H., Jiang, Y., *et al.* (2015) Analysis and Experimental Study of Subsea Connector's Seal Performance. *Journal of Harbin Engineering University*, **36**, 389-393.

[7] Wang, C. and Zhu, H.W. (2013) Structural Property of Bolted Connection Subsea Wellhead Connector. *China Petroleum Machinery*, **41**, 48-52.

[8] Tang, W.X., Cao, W.F., Zhang, J., *et al.* (2016) Performance Analysis of Subsea Wellhead Connector Sealing Structure. *China Petroleum Machinery*, **44**, 82-87.

[9] Zeng, W., Song, H., Xie, H., *et al.* (2019) Sealing Characteristics Analysis of VX Gasket for a Subsea Wellhead Connector Based on Sealing Contact Strength. *Lubrication Engineering*, **44**, 121-126.

[10] Chen, H. (2018) Study on Sealing Structure of the Top Tensioned Riser Hydraulic Connector and Thermal-Structure Coupling Analysis. Master's Thesis, Harbin Engineering University, Harbin.

[11] Standardization Administration of the People's Republic of China (2011) GB150-2011, Pressure Vessels.

[12] Tang, W.X., Cao, W.F., Zhang, J., *et al.* (2016) Performance Analysis of Subsea Wellhead Connector Sealing Structure. *China Petroleum Machinery*, **44**, 82-87.

[13] Li, Y.F., Zhao, H.L., Wang, D.G. and Xu, Y.B. (2020) Metal Sealing Mechanism and Experimental Study of the Subsea Wellhead Connector. *Journal of the Brazilian Society of Mechanical Sciences and Engineering*, **42**, Article No. 26. https://doi.org/10.1007/s40430-019-2112-1

[14] Flitney, R. (2014) Seals and Sealing Handbook. 6th Edition, Butterworth-Heinemann.